Journal of Nuclear and Radiochemical Sciences, Vol. 8, No. 2, pp. 39-45, 2007

Study of Heavy Nuclei at FLNR (Dubna)

Yu. Ts. Oganessian*

Flerov Laboratory of Nuclear Reactions (JINR), 141980 Dubna, Moscow region, Russia

Received: November 13, 2006; In Final Form: February 2, 2007

The synthesis of new nuclides has been performed with the use of the gas-filled recoil separator; in a number of experiments some radio-chemical methods have been employed. The experimental data point to a substantial increase in the nuclear stability with a growing neutron number. For all the nuclei in decay chains undergoing α decay or spontaneous fission the energies and half-lives have been measured. The obtained data are in agreement with predictions of microscopic theory on the deciding role of the nuclear shells in the stability of heaviest elements.

1. Introduction

It is well known that the main field of application of the macroscopic, liquid drop (LD) model has been the description of the average properties of the nuclear masses and deformation energies. From the analysis of the detail properties of heavy nuclei it had become obvious that the macroscopic approaches needed corrections by means of the shell model.[1,2] The main achievements of the macro-microscopic theory are connected with the development of the calculation method of these corrections to the nuclear ground and highly deformed states.[3] In many publications (e.g., see the reviews[4,7–13] and references therein), a number of the existing disagreements between the macroscopic description and experiment were explained by taking into account the shell effect when calculating the nuclear energy in the ground and highly-deformed states (nuclear fission). One important consequence of these calculations was the disclosure of a significant gap in the spectrum of low-lying levels in the region of hypothetical superheavy nuclei, viz. a new (following $N = 126$) closed spherical neutron shell $N = 184$. It was also shown that the considerable variations of the binding energy of spherical nuclei were due to the nuclear shells, and that shell effects might be present also in deformed "magic nuclei" (deformed shells). And finally, at further and quite significant increase of the deformation arising in fission, *the shell effects continued to play an important role* in defining the potential energy and the nuclear inertial masses. The theoretical predictions of above mentioned macro-microscopic approaches, as well as purely microscopic self-consistent models for the new shells, which in fact are not too far from the well known region of the actinides (it is a question of nuclei with mass ~ 280–300), push far away the limits of nuclear masses and extend the region of existing elements at least as far as $Z \sim 120$ and even more.

Of main interest to us are the basic consequences of these models from the point of view of their experimental verification. The remarkable success in the past few years achieved in the synthesis of heavy nuclei in cold fusion reactions are related basically to isotopes in the vicinity of the $N = 162$ shell, mainly at $N < 162$.[14] But in order to probe the effect of the next, spherical shells, which influence a much wider charge and mass region of heavier nuclei, it is necessary to synthesize nuclei with $Z \geq 112$ and $N \geq 172$. This is hard to achieve in cold fusion reactions. One of the key questions pertains to the production of new "magic" nuclei in heavy-ion induced reactions.

*Corresponding author. E-mail: oganessian@jinr.ru.

2. Reactions of Synthesis

In the standard fusion theory, tested in many experiments with light projectiles (from ^{4}He to ^{26}Mg), the evaporation-residues (EVR's) cross section, $\sigma_{\mathrm{EVR}}(E_x) = \Sigma\sigma_{xn}(E_x)$ is determined as

$$\sigma_{xn}(E_x) = \sigma_{\mathrm{CN}}(E_x) \cdot P_{xn}(E_x),$$

where $\sigma_{\mathrm{CN}}(E_x)$ is the cross section for the formation of the compound nucleus with excitation energy E_x, and $P_{xn}(E_x)$ is the probability of its survival during de-excitation by emission of x-nucleons (for the heavy nuclei — mainly neutrons) and γ rays.

It is then assumed that for all collisions with $\ell \leq \ell_{\mathrm{crit}}$, fusion (amalgamation of the interacting nuclei) takes place automatically in a very short time after overcoming the Coulomb barrier. Indeed, if the nuclear attractive force was stronger than the Coulomb repulsion, this simple fusion pattern would be quite defensible. It has been shown also that when the two magic nuclei ^{208}Pb and ^{48}Ca fuse the maximum cross sections for evaporation residues are reached with low excitation energy (cold fusion) and small number of evaporated neutrons ($x = 1$–3).[15] When the projectile becomes more and more heavy, the excitation energy of the compound nuclei decreases (down to $E_x \approx 15$–10 MeV) and the transition to the ground state takes place by the emission of only one neutron and γ rays.[16–18] As a result, the survivability of the compound nucleus $P_{xn}(E_x)$ significantly increases, this being the main advantage of the cold fusion reactions.

Another peculiarity of cold fusion reactions of the nuclei ^{208}Pb or ^{209}Bi with stable isotopes from ^{54}Cr to ^{70}Zn as projectiles lead to the formation of compound nuclei with small neutron excess. The EVR's are some 10–15 mass units shifted from the β-stability line. This, in turn, leads to a considerable decrease in their half-lives. Finally, in cold fusion reactions the six heaviest elements with $Z = 107$–112 were synthesized (see also RIKEN experiment on the synthesis of element 113).[19]

As can be seen from Figure 1(a), the cross section $\sigma_{1n}(Z_{\mathrm{CN}})$ — of the main channel of the synthesis reaction — exponentially decreases with the increase of Z_{CN}. When Z_{CN} changes from 102 to 113 the cross section decreases by almost a factor of 10^7. The observed strong decrease in the cross section with the increase of Z_{CN} in cold fusion points out that strong obstacles arise on the way of formation of the cold compound

Published on Web 10/19/2007

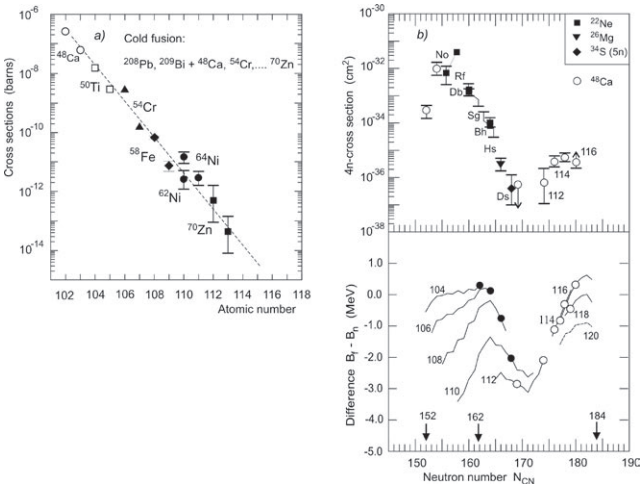

Figure 1. (a) Maximal cross sections of the 1n-evaporation channel in cold fusion reactions. (b) *Upper panel*: experimental cross sections at the maximum of 4n-evaporation channels in hot fusion reactions. *Lower panel*: calculated values of $(B_n - B_f)$ for isotopes of elements 102–120 with different neutron number.

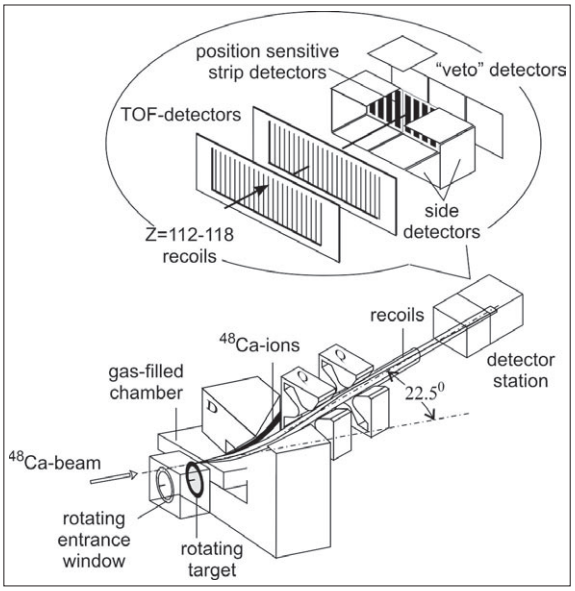

Figure 2. Layout of the Gas-filled Separator.

nucleus itself.

It is clear that the mechanism of fusion of massive nuclei, such as ^{208}Pb and ^{70}Zn, significantly differs from the above-considered simple scenario of formation of compound nuclei using light projectiles. The formation of a composite system of summed mass at the contact point and the following its evolution does not guarantee the formation more compact shape with deformation close to the ground state. This transition is the result of a collective motion of the system in conditions of strong Coulomb repulsion, and the process of formation of the EVR's takes place now via three stages:

$$\sigma_{EVR} = \sigma_{capt} \cdot P_{dyn} \cdot P_{sur}.$$

Experimental data and transport models, describing the stage of collective motion in different assumptions about the dynamical properties of the nuclear system, indicate a strong decrease of P_{dyn} with the increase of the proton number.

In order to decrease the factors hindering fusion, it is desirable to make use of more asymmetric reactions, and to obtain an increase in the neutron number of the EVR's by using both target and projectile nuclei with maximum neutron excess. As target material, it is reasonable to use neutron-rich isotopes of the actinides (Act.), such as ^{244}Pu, ^{248}Cm, and ^{249}Cf, and as projectiles — doubly magic nucleus ^{48}Ca. The compound nucleus ^{292}114, produced, for example, in the fusion of ^{244}Pu and ^{48}Ca, acquires 8 additional neutrons compared to the case of the ^{208}Pb + ^{76}Ge cold fusion reaction. These 8 neutrons, as will be shown below, play a key role in the production and the decay properties of superheavy nuclei. Compared to the cold fusion reaction ^{208}Pb + ^{76}Ge ($Z_P \cdot Z_T = 2624$), the Coulomb repulsion in the reaction ^{244}Pu + ^{48}Ca ($Z_P \cdot Z_T = 1880$) decreases by almost 40%, which, in turn, should lead to the decrease of the factors hindering the formation of a compound nucleus. On the other hand, due to the magic structure of ^{48}Ca, the excitation energy at the Coulomb barrier E_x^{min} of the compound nucleus ^{292}114 amounts to approximately 30 MeV, a value by 10–15 MeV lower than in typical hot fusion reactions induced by lighter projectiles.

The last stage — the survival of the compound nucleus — is the decisive one in the given method of synthesis of the heaviest nuclei.

The estimations of E_x^{min} and the following experiments, aimed to measure the excitation functions for evaporation products, have shown that the compound nuclei with Z_{CN} = 112–118, may attain excitation energy from 30 to 55 MeV. This energy will be released by a cascade emission of 2 to 5 neutrons (the evaporation of charged particles is significantly less probable) and γ rays. Indeed the excitation functions correspond to the evaporation mainly of 3 or 4 neutrons from the excited nucleus, the maximum cross sections for evaporation residues are observed at $E_x \approx 40$ MeV (Reference 20) (hot fusion). The cross sections of nuclei with Z = 102–110, produced in the 4n-evaporation channel of the fusion reactions Act. + ^{22}Ne, ^{26}Mg, and ^{36}S (5n), are presented in Figure 1(b) (the neutron number of the corresponding compound nuclei is shown on the horizontal axis). Since there is no significant hindrance for fusion in such mass-asymmetric reactions ($Z_P \cdot Z_T$ = 920–1500), the strong decrease in the cross section σ_{4n} is connected mainly with the survivability of the nuclei. The relatively high production cross section of isotopes with $Z \leq 105$ is a consequence of the high fission barrier, which is almost completely determined by the shell effect of the two closed neutron shells N = 152 and N = 162. At neutron numbers $N_{CN} > 162$, as can be seen from Figure 1(b) (lower panel) the fission probability significantly increases with the decrease of B_f. However, if the predictions of the theoretical models (see above) about the existence of the next closed shell N = 184 is justified, the fission barrier height will again increase when advancing to the region where $N_{CN} \geq 174$ and $Z_{CN} \geq 112$. In turn, the nuclear survivability will increase too and as a result, one can expect even a rise in the σ_{EVR} for heavy nuclei with large neutron excess. Indeed, as can be seen from the experimental data presented in Figure 1(b), when increasing the number of neutrons from N_{CN} = 169 (^{233}U + ^{48}Ca) to N_{CN} = 172 (^{237}Np + ^{48}Ca) and then to N_{CN} = 178–180 (^{244}Pu,^{248}Cm + ^{48}Ca), σ_{EVR} grows by more than one order of magnitude. For this reason, the observed increase in the survivability of the excited nuclei with neutron number appears to be, to our opinion, evidence for the existence of the closed neutron shell in the region of $N \geq 180$.

3. Setting the Experiments

The Gas-Filled Recoil Separator (DGFRS) used in the experiments with ^{48}Ca projectiles is schematically presented in Figure 2. The calculated and measured in the test experiments transmission efficiency of the separator for Z = 112–118 nuclei is about 35–40%,[21] whereas full-energy ^{48}Ca projectiles, projectile-like ions, and target-like nuclei are suppressed by factors ~10^{17}, 6×10^{14}, and 10^4–10^6, respectively.

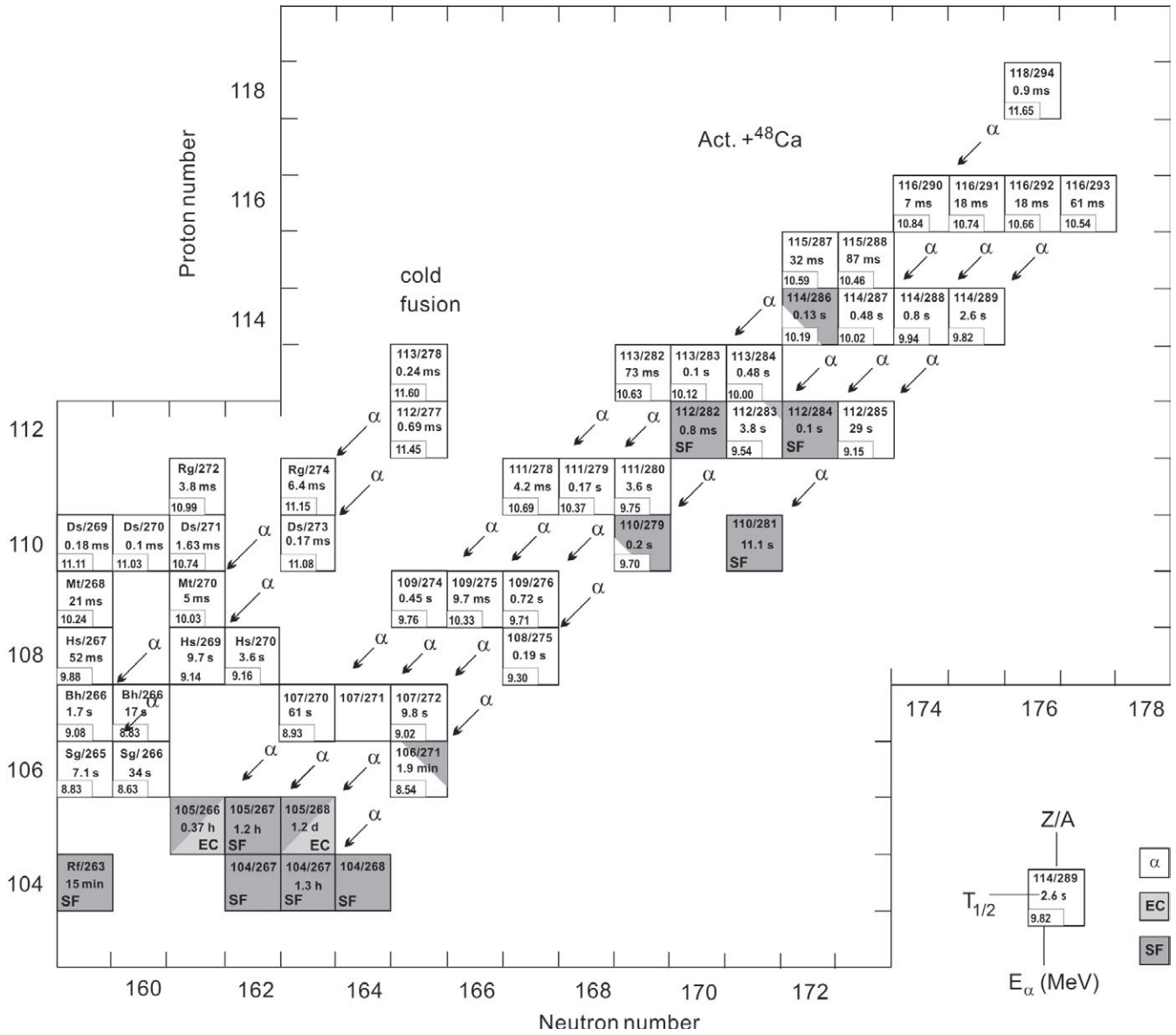

Figure 3. Chart of the heaviest nuclides. The squares contain the half-lives (without errors) and the maximal α-transition energy (E_α in MeV).

The typical beam intensity of ^{48}Ca ions at the target was 1.0–1.2 pμA. The consumption of the ^{48}Ca material amounted to about 0.5 mg/h. In the experiments, targets of actinide oxides of the highly enriched isotopes of U, Np, Pu, Am, Cm, and Cf (thickness of ≈0.35 mg/cm^2) were used.

EVRs passing through the separator were implanted in a 4 × 12-cm^2 semiconductor detector with 12 vertical position-sensitive strips. The detection efficiency of the focal-plane detector array for α-particles is 87% of 4π; for detection one fission fragment — close to 100%, for two fission fragment — about 40%. For α-particles, emitted by the parent or daughter nuclei, it is possible to choose wide enough energy and time gates $\delta E_{\alpha 1}$, $\delta t_{\alpha 1}$ and $\delta E_{\alpha 2}$, $\delta t_{\alpha 2}$ and employ a special low-background detection scheme. An example: during the irradiation of the ^{243}Am target, the beam was switched off after a recoil signal was detected with parameters of implantation energy and TOF expected for evaporation residues, followed by an α-like signal with an energy in the interval $\delta E_{\alpha 1}$ in the same strip/position and a time interval $\delta t_{\alpha 1}$ of up to 8 s. If the first α-particle was not detected (the probability being about 13%), then the switching off the beam was done when a second α-particle in the corresponding $\delta E_{\alpha 2}$ and $\delta t_{\alpha 2}$ intervals was detected. At the registration of the second α-particle the beam-off period is extended to 12 min, whereas of the third — to 3 hours.

Such running condition allowed detection of rare events and decay characteristics of heaviest nuclei with decay time of up to 1 day and even longer.[22] The most short-lived nuclei are detected in DGFRS corresponding to $t \geq 5$ μs. In this way, the setup allows investigation of nuclei in a wide range of half-lives —from 10^{-5} s to more than 10^5 s.

From the characteristics of the DGFRS, which are given above, it follows that with a ^{48}Ca-beam intensity of 1.2 pμA, 0.35 mg/cm^2 target thickness and a beam dose 5 × 10^{18} (realized for 200 hours of operation) the observation of one decay event corresponds to the production cross section of about 0.7 pb.

One of the direct methods of atomic-number identification is based on classical chemical methods, which were long ago used in the first identification and characterization of many of the artificial elements heavier than uranium (see, e.g., Reference 23 and references therein). Obviously, the investigation of the chemical properties of the new nuclides is of separate interest in connection with the study of the structure of superheavy atoms and of the chemical behaviour of the heavy and superheavy elements. Such a possibility is now opened for a series of neutron-rich relatively long-lived nuclei synthesized in Act. + ^{48}Ca reactions. It is seen from Figure 3 that some of nuclei in the decay chains of isotopes with $Z \geq 114$ with odd proton number and/or odd neutron number has a half-lives ranging from several seconds to ~1 day, times — reachable by radiochemical

TABLE 1: Results obtained with DGFRS and in the chemical experiment (^{243}Am + ^{48}Ca)

	DGFRS	Chemical experiment
Separation method	Recoil separator	Radiochemical separation
Separation efficiency	35%	80%
Detection method	Decay chains Z = 115	SF of nuclei with Z = 105
^{48}Ca beam energy	246 MeV	247 MeV
Total ^{48}Ca beam dose	4.3×10^{18}	3.4×10^{18}
Thickness of the ^{243}Am target	0.36 mg/cm^2	1.2 mg/cm^2
Number of detected SF events	3	15
Formation cross section	$2.7^{+4.8}_{-1.6}$ pb	$4.0^{+1.4}_{-1.1}$ pb
Half-life	16^{+19}_{-6} h	32^{+11}_{-7} h
TKE	≈225 MeV	≈230 MeV
Neutron multiplicity / fission		≈4.2
Identification method of SF-decaying nuclei	Excitation functions and decay properties (Z = 115)	Isolation of group 5 elements (Z = 105)

methods. Further below we shall present the results on the chemical isolation of two nuclides: ^{268}Db ($T_{SF} \approx 1.2$ d) and ^{283}112 ($T_\alpha \approx 4$ s). These results are compared with the data from DGFRS.

4. Experimental Results

For the synthesis of superheavy nuclei at DGFRS, the fusion reactions of ^{48}Ca with target nuclei, the isotopes of U, Np, Pu, Am, Cm, and Cf (9 isotopes of six actinide elements), were used. The decay chains are presented in Figure 3. In the investigations carried out at different ^{48}Ca energies, 29 new nuclides (34 including preliminary data for the decay chain of ^{282}113) were detected, all of them being evaporation products and their daughter nuclei in the region of Z = 104–118 and A = 266–294.[20,24]

4.1. Chemical separation of ^{268}Db. As shown above, the longer-lived R-α_1-...-α_5-SF decay chains terminated by a SF nuclide ($T_{SF} = 16^{+19}_{-6}$ h) were associated with the decay of the odd-odd isotope ^{288}115, produced in the 3n-evaporation channel of the ^{243}Am + ^{48}Ca reaction. Since all consecutive α-decays and SF are strongly correlated with each other and the order of occurrence of the nuclei in the decay chains is determined, *the identification of the atomic number of any nucleus in this chain* would independently prove the synthesis of the previously unknown elements 115 and 113.

According to the atomic configuration in the ground state, Db should belong to the 5th group of the Periodic Table, as a heavier homologue of Nb and Ta. The chemical behaviour of Db has been investigated through the study of the 34-s ^{262}Db both in a solution as chloride or fluoride and in the gas phase as volatile bromides and chlorides.[25,26]

For the purpose of chemical identification, Db can be separated, along with the members of chemical group 5, from the other elements. For this case, we developed a method of sorption extraction for the group 5 elements as anionic fluoride complexes. Bearing in mind that the Z = 105 isotope of interest undergoes spontaneous fission, special attention was paid to separating the group 5 elements from the actinides and, most important, from SF isotopes, e.g., ^{252}Cf and ^{254}Cf. Here we shall not give details of the chemical method used for separation of the elements of group 5 (they can be found in the original papers[27–29]), but rather we shall give the main results. It is seen from Table 1 that the decay properties of the long-lived SF nuclei after chemical isolation of Ta fraction from ^{243}Am + ^{48}Ca reaction, in all measured values (T_{SF}, TKE), are consistent with data obtained previously with DGFRS.[22] In this case atomic number of the nuclei of decay chain ^{288}115-$\alpha \rightarrow$ ^{284}113-$\alpha \rightarrow$ ^{280}111-$\alpha \rightarrow$ ^{276}109-$\alpha \rightarrow$ ^{272}107-$\alpha \rightarrow$ ^{268}105 (SF) was confirmed by chemical identification of the long-lived isotope ^{268}Db.

4.2. Chemistry of element 112. The reaction ^{242}Pu(^{48}Ca, 3n)^{287}114-$\alpha \rightarrow$ ^{283}112 was used to produce the isotope ^{283}112. Its cross section, as it follows from experiment (see above), is higher than for the ^{238}U(^{48}Ca,3n)^{283}112 reaction.

The recoil nuclei leaving the ^{242}Pu target stopped in a high-purity gaseous medium: He (70%) + Ar (30%). The energy of the ^{48}Ca beam at the middle of the target was E_{Lab} = 245 MeV, which for a 1.4 mg/cm^2 thick target corresponded to the maximum yield of the isotope ^{287}114 ($T_{1/2} \approx 0.5$ s) — the product of the 3n-evaporation channel of the fusion reaction ^{242}Pu + ^{48}Ca. To the ^{242}Pu target (99.93%) about 15 μg/cm^2 of ^{nat}Nd was added; this allowed to simultaneously produce the neutron-deficient short-lived α-radioactive ^{185}Hg isotope having a half-life of 49 s, which served to monitor the production and separation processes. The recoiling nuclei, which stopped in the He/Ar medium, were transported to the detectors by means of an 8-m capillary tube (the inner diameter was 1.5 mm). The total transport time from the reaction chamber to the detectors was 3.6 s. This time is long enough for the decay ^{287}114 (0.5 s)-$\alpha \rightarrow$ ^{283}112. Also, only about 50% of the daughter nuclides ^{283}112 reached the detector chamber.

The setup COLD[30] consists of 32 pairs detectors, about 1 cm^2 each, placed one opposite the other with a 1.5 mm gap in between, through which the He/Ar gas flows. One of the detectors of each pair was covered with a 30–50-nm gold layer. The temperature gradient along the whole length of the detectors spanned a range from –24 °C to –184 °C in the first experiment and from +35 °C to –180 °C in the second one. The energy resolution for decay α-particles amounted to 120 keV. The SF fission fragment energy was calibrated using a thin ^{248}Cm source.

In the control experiments, only α particles from the decay of $^{181–188}$Hg (the fusion ^{nat}Nd + ^{48}Ca reaction), ^{211}At and ^{219,220}Rn were observed. As it was expected, only nuclei with high volatility were transported to the detectors. It was shown that all Hg atoms are registered by the first detectors with the Au coating. This can be explained by the strong adsorption on the detector Au-surface, which is due to the chemical reaction leading to the production of the Hg/Au compound. On the contrary, the decay of the chemically neutral Rn atoms is observed in the region of the last detectors, which are at the lowest temperatures (Figure 4). In these conditions, the atoms of element 112 must be between these two extreme cases, their position (detector number) depending on their chemical properties.

Two events from the decay of ^{283}112 were observed in the detector chamber (Figure 4). In the first case, the sequence α-SF with $E_\alpha = 9.38 \pm 0.12$ MeV and then 0.59 s later the two fragments with total kinetic energy TKE = 231 MeV were registered by the second pair of detectors with the Au surface at

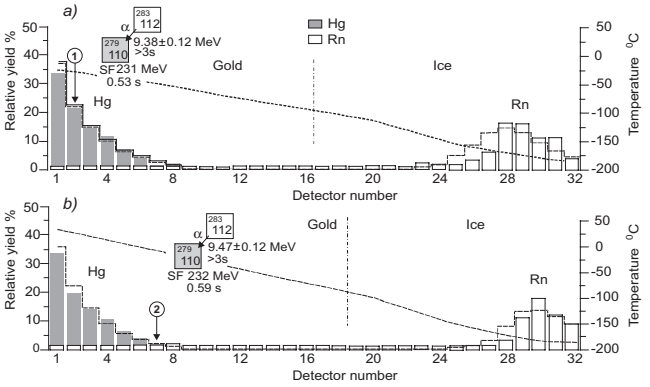

Figure 4. Results of thermo-chromatographic separation of element 112, produced in the reaction ^{242}Pu(^{48}Ca,3n)^{287}114-$\alpha \rightarrow ^{283}$112. The dotted lines (right-hand axis) denote the temperature distribution along the 32 detectors from the two experiments. The relative yields of the 49 s-^{185}Hg and 3.7 s-^{219}Rn are shown together with the observed decays of 3.8 s-^{283}112 (black arrows) as a function of the detector number. The Monte Carlo simulation of the adsorption process of Hg and Rn on the gold surface and ice are shown by the red dashed line. (a) the temperature gradient is –24 °C to –184 °C; (b) the temperature gradient +35 °C to –180 °C. Figure is taken from Reference 31.

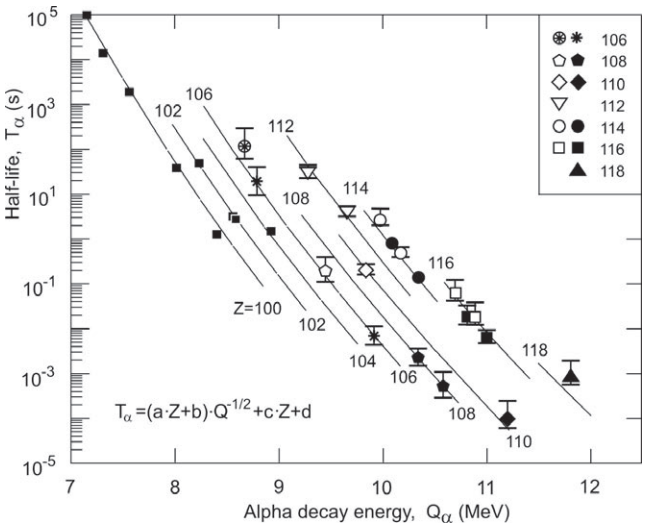

Figure 5. Half-lives T_α as a function of the α-decay energy Q_α for nuclei with even atomic numbers $Z \geq 100$ (indicated in the figure). The solid lines represent calculations using the Viola-Seaborg formula (given in the figure). The black symbols denote even-even isotopes, the open symbols — even-odd.

temperature –28 °C (the temperature conditions for detectors 1 to 32 were in the range –24 °C to –184 °C). In the second case, the same α-SF sequence (E_α = 9.47 ± 0.12 MeV, t_{SF} = 0.54 s, TKE = 232 MeV) was registered by the seventh detector pair again on the Au surface, which was at –5 °C (the temperature conditions for detectors 1 to 32 were in the range +35 °C to –180 °C). Both events are consistent with the properties of the decay of the ^{283}112 nucleus. While the first event practically follows the location of the Hg atoms the second one somewhat differs (the probability of Hg hitting the 7th detector is about 3%). This may mean weaker adsorption of element 112 with gold compared to Hg, but it is obviously stronger than expected for noble-gas like behaviour. Avoiding the details, they are given in a separate publication[31] (experiments with the isotopes ^{283}112 and ^{285}112 are continued), even now from the obtained data a conclusion can be drawn that the isotope ^{283}112 by its chemical properties is related to the group 12 elements. The production cross section of ^{283}112 in the reaction ^{242}Pu(^{48}Ca,3n)^{287}114-$\alpha \rightarrow ^{283}$112 is estimated as 2–4 pb depending on the adsorption properties of the parent nucleus ^{287}114 at room temperature (from the DGFRS measurements $\sigma_{3n} = 3.6^{+3.4}_{-1.7}$ pb).[28] The results of the given experiment in an independent way confirm the identification of the atomic numbers of the nuclides in the even-Z nuclear decay chain ^{291}116 $\rightarrow$ ^{287}114 $\rightarrow$ **^{283}112** $\rightarrow$ ^{279}110 $\rightarrow$ ^{275}108 $\rightarrow$ ^{271}106 $\rightarrow$ ^{267}104.

5. Discussions

Actually the identification of the atomic numbers of the nuclides was performed by:

- the mechanism of fusion reactions (excitation functions and cross bombardments ensuring variation of the proton and neutron numbers of the compound nucleus);
- decay properties of the nuclei in the decay sequences (half-lives T_α and α-decay energies Q_α of even-even (and for many even-odd) isotopes; see Figure 5;
- radiochemical identification of the atomic number of the nuclides ^{268}Db and ^{283}112 — links of the decay chains of the parent nuclei: ^{288}115 and ^{291}116.[27–29,31]

All methods give the same identification of the atomic number of the synthesized nuclei. When the atomic numbers of the parent nuclei are determined (showing that they are the products of xn-evaporation channels), the identification of the mass of an isotope comes to the quantification of evaporated neutrons at various excitation energies. This is achieved:

- by means of the measured excitation functions ensuring variation of the neutron number in the compound nucleus;
- by producing the same nuclei in different ways: as evaporation residues and as α-decay products of heavier nuclei.

The adjoining four isotopes of the elements with Z = 112, 114, and 116, genetically connected with the daughter nuclei by consecutive α decays give a self-consistent picture of the atomic and mass numbers of all nuclides, synthesized in the ^{48}Ca-induced experiments.

Further verification of the identification of the mass number of the isotopes follows from the decay properties. Because of the high suppression of spontaneous fission of nuclei with odd neutron numbers, their decay chains are longer and the total decay time is noticeably higher than those in the neighbouring even-N isotopes (see chains on the Figure 3).

5.1. Alpha decay. As can be seen from Figure 3, the odd isotopes of element 112 and all isotopes (even and odd) with $Z \geq 113$ predominantly undergo α decay. As known from the theory of α decay, in this case the probability for the decay (or the half-life T_α) is directly connected to the decay energy Q_α and the atomic number of the nucleus. The experimental values obtained earlier in hot and cold fusion reactions and belonging to the α decay of even-even nuclei with $100 \leq Z \leq 110$ with new data for all isotopes with even proton numbers from Z = 106 to 118, produced in ^{48}Ca-induced reactions, are shown in Figure 5. The experimental values Q_α(exp) and T_α(exp) shows steep raise of the T_α with increase the neutron number in heaviest nuclei. They can be used also for the calculation of the atomic numbers of nuclei comprising the chains of correlated decays. For example the probability that the consecutive α transitions observed in the ^{245}Cm,^{248}Cm + ^{48}Ca reaction take place in the nuclei with atomic numbers 116 $\rightarrow$ 114 $\rightarrow$ 112 $\rightarrow$ 110 amounts to 0.992.

The values of Q_α(th), obtained in the framework of the macroscopic-microscopic (MM) model in the version of Reference 32 for the isotopes of all elements with even atomic numbers from Z = 100 to 118 and with odd atomic numbers from Z = 103 to 115, are presented in Figures 6(a) and 6(b), respectively. The predicted Q_α(th) values for the heaviest nuclei, observed in our experiments are systematically larger than the experimental data.

At the same time, the trends of the predictions are in good agreement for the 23 nuclides with Z = 106–118 and N = 165–

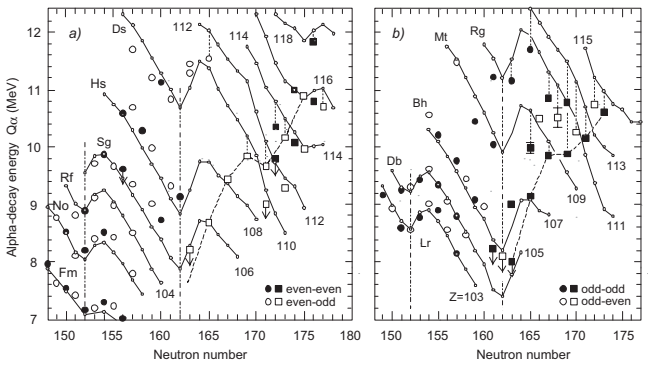

Figure 6. Alpha-decay energy vs. neutron number for: (a) the isotopes of even-Z elements with $Z \geq 100$, (b) isotopes of odd-Z elements with $Z \geq 103$. Squares correspond to the nuclei, produced in ^{48}Ca-induced reactions. Dashed lines are long sequences of correlated decays of the nuclei ^{288}115 and ^{291}116. The solid lines are Q_α(th), calculated in the MM model.

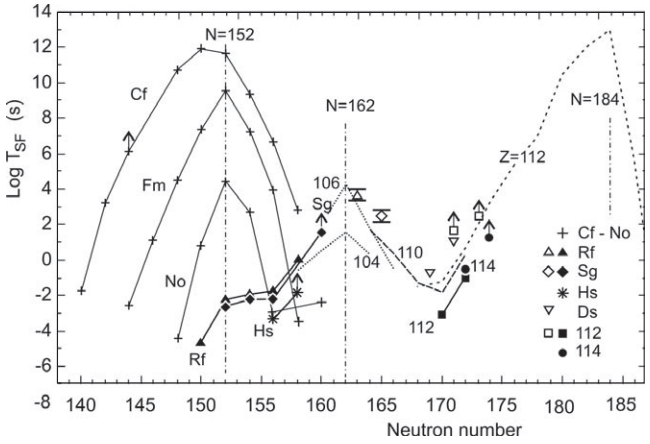

Figure 7. Partial half-lives for spontaneous fission T_{SF} vs. N for nuclei with even Z = 98–114. Solid symbols and crosses denote even-even nuclei, open symbols — even-odd. Solid lines are drawn through the experimental points of even-even nuclei, the dashed lines — calculated T_{SF}(th).

177. The trend of the $Q_\alpha(N)$ systematics, predicted by theory and confirmed by experimental data can be considered *as direct evidence for the deformed neutron shell closure at N = 162*.

The comparison of Q_α(exp) with the values Q_α(th), calculated within the Skyrme-Hartree-Fock Bogoliubov (HFB) and the Relativistic Mean Field models (RMF), was carried out, too. In the HFB model a better agreement is obtained with masses from Reference 33 calculated with 18 parameters. Finally, in the RMF model the agreement between theory and experiment is least satisfactory. But it cannot be excluded that a better agreement can be achieved in this model also by using a different set of parameters.

As a whole, the measured values of Q_α(exp) are in agreement with theory, because the model calculations do not claim to be more precise in determining Q_α(th) than 0.4–0.6 MeV. We must recall, that all three models predict the same spherical neutron shell at N = 184, but different proton shells, Z = 114 (MM) and Z = 120, 124, or 126 (HFB, RMF). Yet, all describe the experimental data equally well. Such insensitivity with respect to the various models in this region of Z and N can be explained either by the remoteness of the nuclei under consideration from the closed shell at N = 184 or by the weaker influence of the proton shells at Z = 114 or higher, compared to that of the neutron shell at N = 184.

5.2. Spontaneous fission. For 8 out of the 34 synthesized nuclei spontaneous fission is the predominant mode of decay. In two more nuclei, ^{271}Sg and ^{286}114, spontaneous fission competes with α decay. For the remaining nuclides spontaneous fission was not observed. The partial SF half-lives of nuclei with $N \geq 163$, produced in fusion reactions with ^{48}Ca, together with the half-lives of SF nuclides with $N \leq 160$, are shown in Figure 7.

Four isotopes of element 112 with N = 170–173 are located in a region, where a steep rise of $T_{SF}(N)$ is expected. Indeed, in the even-even isotopes ^{282}112 and ^{284}112 the difference of two neutrons increases the partial half-life T_{SF} by two orders of magnitude.

The neighbouring odd isotopes ^{283}112 and ^{285}112 undergo α decay. For them, only lower limits of T_{SF} can be determined (shown in the figure). Such a picture is observed also for the even-even isotopes of element 114: the additional two neutrons in the nucleus ^{286}114 ($T_{SF} \approx 0.13$ s) lead to increase of the stability relative to spontaneous fission. It is significant that the rise of stability relative to spontaneous fission is observed for the nuclei are by 10–12 neutrons away from the closed neutron shell N = 184.

For the nuclei with $Z < 110$ and $N < 170$ the probability for spontaneous fission decreases again when the deformed shell closure N = 162 is approached. The stabilizing effect of the N = 162 shell manifests itself in the properties of the even-even isotopes of Rf, Sg, and Hs with $N \leq 160$, which, as seen from Figure 7, are well described by the mentioned model calculations. The odd SF-isotopes with Z = 104–110, produced in the ^{48}Ca-induced reactions, are located in the transition region, where the larger the neutron number, the smaller the effect of the N = 162 shell. In this region, the N = 184 shell comes into effect. Such a behaviour of T_{SF}(exp) as a function of Z and N correlates with the SHE fission barrier heights and has been predicted by all models: MM, HFB, and RMF. For the isotopes of element 115, due to the strong hindrances to spontaneous fission of nuclei with odd proton (or/and neutron) number, α decay predominates as far as the N = 162 shell, where, similarly to the previous case, the sequences terminates by spontaneous fission.

The decay properties of the nuclei obtained in Act. + ^{48}Ca reactions show that the basic theoretical concept on the existence of closed shells in the region of the hypothetical superheavy elements and their decisive role in defining the limits of nuclear mass has received its experimental confirmation.

The experiments were performed at U-400 heavy ion cyclotron of the FLNR (JIINR) in collaboration with Analytical and Radiochemical Division of LLNL (USA); the experiments on the chemical identification of the isotopes ^{268}Db and ^{283}112 within the collaboration: Paul Scherrer Institute (PSI, Villigen), Department for Chemistry and Biochemistry of the University of Bern, Institute of Electronic Technology (IET, Warsaw) with the participation of Dr. M. Hussonois from the Institute of Nuclear Physics (IPN, Orsay).

References

(1) O. Haxel, J. H. Jensen, and H. E. Suess, Phys. Rev. **75**, 1766 (1949).
(2) M. G. Mayer, Phys. Rev. **75**, 1969 (1949).
(3) V. M. Strutinski, Nucl. Phys. **A95**, 420 (1967); Nucl. Phys. **A122**, 1 (1968).
(4) M. Brack, J. Damgaard, A. S. Jensen, H. C. Pauli, V. M. Strutinsky, and C. Y. Wong, Rev. Mod. Phys. **44**, 320 (1972).
(5) S. G. Nilsson, C. F. Tsang, A. Sobiczewski, Z. Szymański, S. Wycech, C. Gustafson, I.-L. Lamm, P. Möller, and B. Nilsson, Nucl. Phys. **A131**, 1 (1969).
(6) B. Mottelson and S. G. Nilsson, Phys. Rev. **99**, 1615 (1955).

(7) A. Sobiczewski, F. A. Gareev, and B. N. Kalinkin, Phys. Lett. **22**, 500 (1966).
(8) H. Meldner, Ark. Fys. **36**, 593 (1967).
(9) U. Mosel and W. Greiner, Z. Phys. **222**, 261 (1969).
(10) P. Möller and J. R. Nix, J. Phys. G **20**, 1681 (1994).
(11) A. Sobiczewski, Phys. Part. Nucl. **25**, 119 (1994).
(12) W. Greiner, Int. J. Mod. Phys. E **5**, 1 (1995).
(13) R. Smolańczuk, J. Skalski, and A. Sobiczewski, Phys. Rev. C **52**, 1871 (1995).
(14) S. Hofmann, Rep. Prog. Phys. **61**, 639 (1998).
(15) G. N. Flerov, Yu. Ts. Oganessian, A. A. Pleve, N. V. Pronin, and Yu. P. Tretyakov, Nucl. Phys. **A267**, 359 (1976).
(16) P. Armbruster, Ann. Rev. Nucl. Part. Sci. **35**, 135 (1985).
(17) G. Münzenberg, Rep. Prog. Phys. **51**, 57 (1988).
(18) S. Hofmann and G. Münzenberg, Rev. Mod. Phys. **72**, 733 (2000).
(19) K. Morita, K. Morimoto, D. Kaji, T. Akiyama, S. Goto, H. Haba, E. Ideguchi, R. Kanungo, K. Katori, H. Koura, H. Kudo, T. Ohnishi, A. Ozawa, T. Suda, K. Sueki, H. S. Xu, T. Yamaguchi, A. Yoneda, A. Yoshida, and Y. L. Zhao, J. Phys. Soc. Jpn. **73**, 2593 (2004).
(20) Yu. Ts. Oganessian, V. K. Utyonkov, Yu. V. Lobanov, F. Sh. Abdullin, A. N. Polyakov, I. V. Shirokovsky, Yu. S. Tsyganov, G. G. Gulbekian, S. L. Bogomolov, B. N. Gikal, A. N. Mezentsev, S. Iliev, V. G. Subbotin, A. M. Sukhov, A. A. Voinov, G. V. Buklanov, K. Subotic, V. I. Zagrebaev, M. G. Itkis, J. B. Patin, K. J. Moody, J. F. Wild, M. A. Stoyer, N. J. Stoyer, D. A. Shaughnessy, J. M. Kenneally, and R. W. Lougheed, Phys. Rev. C **69**, 054607 (2004); Phys. Rev. C **70**, 064609 (2004).
(21) K. Subotic, Yu. Ts. Oganessian, V. K. Utyonkov, Yu. V. Lobanov, F. Sh. Abdullin, A. N. Polyakov, Yu. S. Tsyganov, and O. V. Ivanov, Nucl. Instrum. Methods Phys. Res. A **481**, 71 (2002).
(22) Yu. Ts. Oganessian, V. K. Utyonkov, Yu. V. Lobanov, F. Sh. Abdullin, A. N. Polyakov, I. V. Shirokovsky, Yu. S. Tsyganov, G. G. Gulbekian, S. L. Bogomolov, B. N. Gikal, A. N. Mezentsev, S. Iliev, V. G. Subbotin, A. M. Sukhov, O. V. Ivanov, G. V. Buklanov, K. Subotic, M. G. Itkis, J. B. Patin, K. J. Moody, J. F. Wild, N. J. Stoyer, M. A. Stoyer, D. A. Shaughnessy, J. M. Kenneally, and R. W. Lougheed, Phys. Rev. C **69**, 021601 (2004).
(23) E. K. Hyde, I. Perlman, and G. T. Seaborg, *The Nuclear Properties of the Heavy Elements, Detailed Radioactive Properties*, Prentice-Hall, Inc., Englewood Cliffs, New Jersey (1964).
(24) Yu. Ts. Oganessian, V. K. Utyonkov, Yu. V. Lobanov, F. Sh. Abdullin, A. N. Polyakov, I. V. Shirokovsky, Yu. S. Tsyganov, G. G. Gulbekian, S. L. Bogomolov, B. N. Gikal, A. N. Mezentsev, S. Iliev, V. G. Subbotin, A. M. Sukhov, O. V. Ivanov, G. V. Buklanov, K. Subotic, M. G. Itkis, K. J. Moody, J. F. Wild, N. J. Stoyer, M. A. Stoyer, and R. W. Lougheed, Phys. Rev. C **62**, 041604(R) (2000); Phys. Rev. Lett. **85**, 3154 (1999); Yad. Fiz. **63**, 1769 (2000) [Phys. At. Nucl. **63**, 1679 (2000)]; Phys. Rev. C **63**, 011301(R) (2001); Nucl. Phys. A **734**, 109 (2004); Phys. Rev. C **72**, 034611 (2005); Phys. Rev. C **74**, 044602 (2006).
(25) W. Paulus, J. V. Kratz, E. Strub, S. Zauner, W. Brüchle, V. Pershina, M. Shädel, B. Shausten, J. L. Adams, K. E. Gregorich, D. C. Hoffman, M. R. Lane, C. Laue, D. M. Lee, C. A. McGrath, D. K. Shaughnessy, D. A. Strellis, and E. R. Sylwester, Radiochim. Acta **84**, 69 (1999).
(26) H. W. Gäggeler and A. Türler, *The Chemistry of Superheavy Elements,* Ed. M. Schädel, Kluwer Academic Publisher, Dordrecht (2003), p 237; J. V. Kratz, ibid., p 159.
(27) S. N. Dmitriev, Yu. Ts. Oganessyan, V. K. Utyonkov, S. V. Shishkin, A. V. Yeremin, Yu. V. Lobanov, Yu. S. Tsyganov, V. I. Chepygin, E. A. Sokol, G. K. Vostokin, N. V. Aksenov, M. Hussonnois, M. G. Itkis, H. W. Gäggeler, D. Schumann, H. Bruchertseifer, R. Eichler, D. A. Shaughnessy, P. A. Wilk, J. M. Kenneally, M. A. Stoyer, and J. F. Wild, Mendeleev Commun. **15**, 1 (2005).
(28) D. Schumann, H. Bruchertseifer, R. Eichler, B. Eichler, H. W. Gäggeler, S. N. Dmitriev, Yu. Ts Oganessian, V. P. Utyonkov, S. V. Shishkin, A.V. Yeremin, Y. V. Lobanov, Yu. S. Tsyganov, V. I. Chepygin, E. A. Sokol, G. I. Vostokin, N. V. Aksenov, M. Hussonois, and M. G. Itkis, Radiochim. Acta **93**, 727 (2005).
(29) N. J. Stoyer, J. H. Landrum, P. A. Wilk, K. J. Moody, J. M. Kenneally, D. A. Shaughnessy, M. A. Stoyer, J. F. Wild, R. W. Lougheed, S. N. Dmitriev, Yu. Ts. Oganessian, S. Shishkin, N. Aksenov, E. Tereshatov, G. Bozhikov, V. Utyonkov, and A. Yeremin, *Proc. IX Int. Conf. on Nucleus-Nucleus Collisions, Rio de Janeiro, Brazil, August 28–September 1, 2006* (to be published).
(30) Ch. E. Düllmann, B. Eichler, R. Eichler, H. W. Gäggeler, D. T. Jost, D. Piguet, and A. Türler, Nucl. Instrum. Methods Phys. Res. A **479**, 631 (2002); S. Soverna, R. Dressler, Ch. E. Düllmann, B. Eichler, R. Eichler, H. W. Gäggeler, F. Haenssler, J.-P. Niklaus, D. Piguet, Z. Qin, A. Türler, and A. B. Yakushev, Radiochim. Acta **93**, 1 (2005).
(31) R. Eichler, N. V. Aksenov, A. V. Belozerov, G. A. Bozhikov, V. I. Chepigin, R. Dressler, S. N. Dmitriev, H. W. Gäggeler, V. A. Gorshkov, F. Haenssler, M. G. Itkis, V. Ya. Lebedev, A. Laube, O. N. Malyshev, Yu. Ts. Oganessian, O. V. Petrushkin, D. Piguet, P. Rasmussen, S. V. Shishkin, A. V. Shutov, A. I. Svirikhin, E. E. Tereshatov, G. K. Vostokin, M. Wegrzecki, and A. V. Yeremin, Nature **447**, 72 (2007).
(32) I. Muntian, Z. Patyk, and A. Sobiczewski, Acta Phys. Pol. B **34**, 2073 (2003); Phys. At. Nucl. **66**, 1015 (2003).
(33) S. Goriely, M. Samyn, P.-H. Heenen, J. M. Pearson, and F. Tondeur, Phys. Rev. C **66**, 024326 (2002).